Erosion Model for Brittle Materials Under Low-Speed Impacts

Zhen-Ting Wang
Northwest Institute of Eco-Environment and Resources, CAS,
Lanzhou 730000, China
Email: wangzht@lzu.edu.cn

The erosion of perfectly brittle materials under low-speed impacts is studied by the combination of the Hertzian contact theory and the maximum stress criterion. It is found that the fractional erosion per impact is proportional to the product of the square root of the yield strain and the ratio of the kinetic energy per volume of the impacting body to the critical strain energy density of the target. The novel formula is conceptually extended to the erosion of cracked brittle materials. [DOI: 10.1115/1.4046019]

Keywords: abrasion, contact, contact mechanics, erosion

1 Introduction

The tribological term of erosion refers to the wear by solid particle impingements [1]. For brittle targets, it is well-known that cracks can form and propagate when the impact speed reaches a threshold [2]. Therefore, fracture mechanics has been frequently used to predict the mass or volume removal by an impacting particle, e.g., Refs. [3,4], since the early attempt of Sheldon and Finnie [5,6]. A theoretical estimation shows that the minimum impact speed to cause surface yield is only 0.14 m/s for a hard steel sphere striking a medium-hard steel body [7]. Does the erosion of brittle materials without the emergence of cracks occur under low-speed impacts? Yes, this is a real process although the instantaneous or short-term damage might be invisible or little. Rocks are often regarded as an ideally brittle material in fracture mechanics [8], as well as glasses, ceramics, and ice. In arid, coastal, and periglacial environments on earth, wind-carried solid particles can slowly shape many types of rocks, such as basalt, marble, carbonate, and dolerite etc., to form ventifacts with one or more facets separated by sharp keels over long time periods [9–12]. Another common erosive morphological feature in arid environments is yardangs, often having beautiful streamlined shapes [13,14]. Our knowledge of Mars has been advanced extraordinarily over the past several decades. As an active geological process on the current Martian surface, wind erosion has sculpted abundant landforms analogous to terrestrial ventifacts and yardangs [15–17]. The accurate prediction of the erosion rate is crucial to understand the evolution of these aeolian features. It is experimentally found that erosion rate is proportional to the kinetic energy of impacting particles [18]. Subsequently, the Young's modulus and yield stress of target materials are theoretically introduced into this empirical formula [19,20]. One weakness of the later works is that the contact area during impact is replaced with a point. In this study, another simple expression for erosion rate is derived according to the more rigorous Hertzian contact theory.

2 Model

The perpendicular collision between a rigid sphere and a half-space consisted of a pure brittle material is a special case of the collinear impact of two elastic spheres. Assuming that the contact area is small when compared with the dimensions of the impacting sphere, the following maximum compression δ_* is obtained from the motion equation of the Hertzian theory [7,21],

$$\delta_* = \left(\frac{15mv_0^2}{16R^{1/2}E}\right)^{2/5} \tag{1}$$

where m, R, and v_0 are the mass, radius, and initial speed of the sphere and E is the Young's modulus of the half-space.

The corresponding maximum contact radius a_* and pressure p_* are

$$a_* = \sqrt{R\delta_*} \tag{2}$$

and

$$p_* = \frac{2a_*E}{\pi R} \tag{3}$$

The volume removal is taken to be proportional to the volume bounded by the outermost ring crack around the contact area and the depth of the initial crack in the crack-based method [22]. Analogously, the erosion volume V per impact is estimated as

$$V \propto a^2 h \tag{4}$$

where a and h are the maximum radius and depth where the target material reaches its elastic limit.

The stress field within the half-space and failure criterion must be provided to compute a and h. The maximum stress criterion is often utilized to predict the failure of brittle materials. For simplicity, the uniaxial tension and compression strengths are denoted by the same symbol of σ_s. The detailed expressions of stress components can be found in Ref. [7]. The tensile stress outside the contact circle determines the maximum radius a of failure

$$\frac{1-2\nu}{3}\left(\frac{a_*}{a}\right)^2 p_* = \sigma_s \tag{5}$$

where ν is the Poisson's ratio of the target material.

There is no impact erosion if the maximum tensile stress occurring at the edge of the contact area is less than σ_s. When $a = a_*$, Eqs. (1)–(3) and (5) determine the threshold impacting speed,

$$v_0^* = \left(\frac{4E}{5\pi\rho}\right)^{1/2}\left[\frac{3\pi\sigma_s}{2(1-2\nu)E}\right]^{5/2} \tag{6}$$

where ρ is the density of the impacting sphere.

The compressive stress along the symmetric axis gives the equation of the maximum depth h of failure,

$$1 + \left(\frac{h}{a_*}\right)^2 = \frac{p_*}{\sigma_s} \tag{7}$$

When $p_*/\sigma_s \gg 1$, Eq. (7) reduces to

$$h \propto \left(\frac{p_*}{\sigma_s}\right)^{1/2} a_* \tag{8}$$

Combining Eqs. (4), (5), and (8), we have,

$$V \propto \left(\frac{p_*}{\sigma_s}\right)^{3/2} a_*^3 \tag{9}$$

Substituting Eqs. (1)–(3) into Eq. (9), the volume removal is

$$V \propto R^3\left(\frac{\rho v_0^2}{E}\right)^{9/10}\left(\frac{E}{\sigma_s}\right)^{3/2} \tag{10}$$

Since particle size is often described by diameter $d = 2R$ rather

Contributed by the Tribology Division of ASME for publication in the Journal of Tribology. Manuscript received November 1, 2019; final manuscript received January 7, 2020; published online January 17, 2020. Assoc. Editor: Yun-Bo Yi.

than the radius and 9/10 in Eq. (10) is very close to 1, we get,

$$\frac{V}{d^3} \propto \frac{\rho v_0^2}{E}\left(\frac{E}{\sigma_s}\right)^{3/2} = \frac{\rho v_0^2 E}{\sigma_s^2}\left(\frac{\sigma_s}{E}\right)^{1/2} \tag{11}$$

The contact pressure is calculated under the assumption that each body can be regarded as an elastic half-space [7]. Hence, Eq. (11) is also suitable for the erosion of a brittle sphere normally impacting a rigid wall.

3 Results and Discussion

It is necessary to explain the physical meanings of formulae first. The non-dimensional term of $A_1 = \rho v_0^2 E/\sigma_s^2$ in the right side of Eq. (11) represents the ratio of the kinetic energy per volume of the impacting sphere to the critical strain energy density of the brittle target. It has been derived in a more complicated manner [19]. It should be pointed out that the model of Sheldon and Finnie [5] can be simplified to a similar expression of A_1 when the flaw distribution parameter is large enough. The novel expression of $A_2 = A_1(\sigma_s/E)^{1/2}$ further reflects the effect of yield strain.

Are A_1 and A_2 practical? An apparatus was designed and constructed to measure the erosion rate of various rocks [15,18]. The control of most dominant parameters such as impact velocity, impact angle, impacting grain size, target type, and atmospheric density, etc. was realized. A series of impact erosion experiments were performed by Greeley et al. [18] for the detailed experimental procedure. One of them is that $125 \sim 180$ μm quartz grains normally impact a wide range of target materials including basalt, obsidian, rhyolite, gypsum cement, and brick, etc. Unfortunately, the mechanical behaviors of these targets were not measured simultaneously. Here, the data of basalt and rhyolite are selected to test the above-mentioned model, because the mechanical parameter ranges of these two rocks are narrow. The values of Young's modulus and yield strength are $E = 89$ GPa, $\sigma_s = 71$ MPa for basalt, $E = 26$ GPa, $\sigma_s = 45$ MPa for rhyolite [19]. As shown in Fig. 1, the experimental data can be well fitted by the theoretical non-dimensional parameters of A_1 and A_2. This indicates that the yield strain effect contained in A_2 might be insignificant for brittle targets. There is a fundamental difference between A_1 and A_2. For A_1, the threshold impacting speed v_0^* is zero because the stress field at the unique contact point is singular [19]. It is estimated from Eq. (6) that $v_0^* = 0.025$ m/s for basalt and 0.094 m/s for rhyolite while $\rho_s = 2.65 \times 10^3$ kg/m^3 and $\nu = 0.3$. The threshold impacting speeds are so small that the applications of A_1 and A_2 do not differ greatly. Although the object of our study is aeolian erosive features, the obtained erosion ratio expressions also apply to bedrock erosions by solid particles in coastal and fluvial environments because their solid-to-solid contact and damage processes are similar.

Finally, let us compare the presented work with other models. There are many wear models using different variables and mechanical parameters [23]. For perfectly brittle materials, Young's modulus and yield strength are sufficient. Assuming that the contact pressure is equivalent to the yield stress, another form of the fractional erosion per impact can be derived [24]. When $\rho v_0^2 \gg \sigma_s$, it reduces to $\rho v_0^2/\sigma_s$ which is more simple than A_1 or A_2. For cracked brittle materials, the crack extension is governed by the critical stress intensity factor, also known as fracture toughness. The crack instability problem of a large plate containing a crack subjected to a remote and uniform tensile load perpendicular to the crack line has been solved by the Griffith crack theory [25]. The fracture toughness is expressed as

$$K_c = \sigma_s\sqrt{\pi l} \tag{12}$$

where l is the one-half crack length.

Different from the Hertzian contact in which $a_* \ll d$, the crack length could be scaled with the impacting sphere,

$$l \sim d \tag{13}$$

Replacing σ_s in A_1 with K_c, we get a dimensionless parameter,

$$\eta = \frac{\rho v_0^2 E d}{K_c^2} \tag{14}$$

It is interesting that η is analogous with the fractional erosion developed for semi-brittle materials by Ghadiri and Zhang [4]. The later is,

$$\eta = \frac{\rho v_0^2 H d}{K_c^2} \tag{15}$$

where H is the hardness. Compared with Eq. (14), the Young's modulus E disappears, because the contact time in their model is estimated by plastic flow rather than elastic deformation. The hardness H is commonly several times of the yield stress σ_s. For perfectly brittle materials, Eq. (15) also reduces to $\rho v_0^2/\sigma_s$.

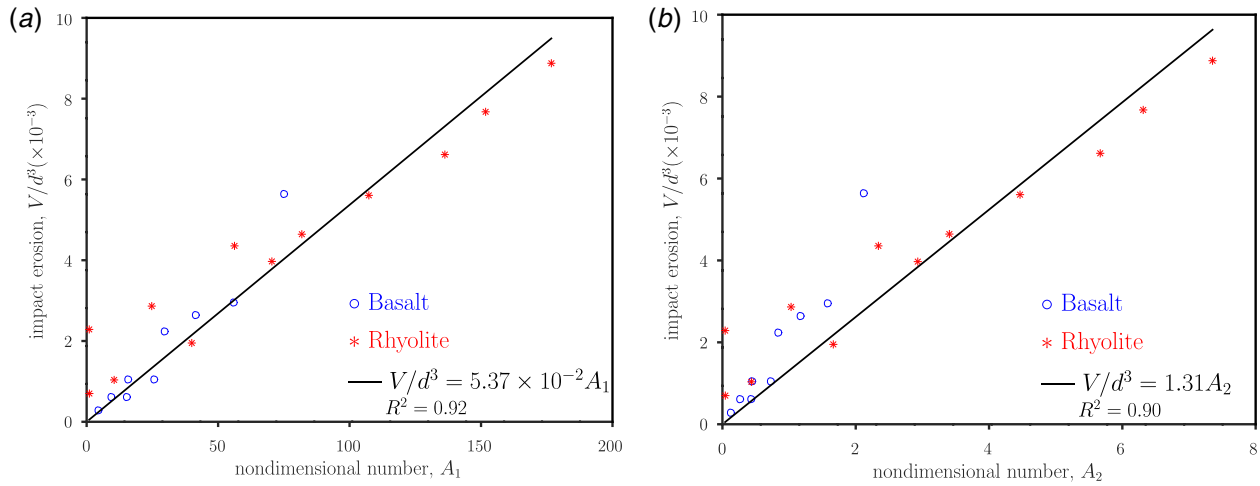

Fig. 1 Comparison between experiment and theory. The longitudinal coordinate is V/d^3 multiplied by an unknown constant. The data can be well fitted by the non-dimensional parameters of A_1 and A_2: (a) change of impact erosion with A_1 and (b) change of impact erosion with A_2.

4 Conclusions

The Hertzian contact theory leads to a simple erosion expression for the perfectly brittle materials under low-speed impacts. The novel dimensionless parameter reflects the ratio of the kinetic energy per volume of the impacting sphere to the target's critical strain energy density plus the yield strain effect. It can be extended to the erosion of cracked brittle materials conceptually. This theoretical work provides an alternative formula for the fractional erosion per impact, different from the previous models established under the assumption of pure plastic deformation during impacts.

Acknowledgment

This research was supported by the Natural Science Foundation of China projects (Nos. 41630747 and 41971011) and the State Key Laboratory of Desert and Oasis Ecology Project (No. G2018-02-01).

References

[1] Ludema, K. C., and Ajayi, L., 2019, *Friction, Wear, Lubrication: a Textbook in Tribology*, 2nd ed., Taylor & Francis, CRC Press, Boca Raton.
[2] Huang, Z., Li, G., Tian, S., Song, X., Sheng, M., and Shah, S., 2018, "Theoretical Basis of Abrasive Jet," *Abrasive Water Jet Perforation and Multi-Stage Fracturing*, Elsevier, Cambridge, pp. 1–62.
[3] Evans, A. G., Gulden, M. E., and Rosenblatt, M., 1978, "Impact Damage in Brittle Materials in the Elastic-Plastic Response Regime," Proc. R. Soc. A: Math., Phys. Eng. Sci., **361**(1706), pp. 343–365.
[4] Ghadiri, M., and Zhang, Z., 2002, "Impact Attrition of Particulate Solids. Part 1: A Theoretical Model of Chipping," Chem. Eng. Sci., **57**(17), pp. 3659–3669.
[5] Sheldon, G. L., and Finnie, I., 1966, "The Mechanism of Material Removal in the Erosive Cutting of Brittle Materials," ASME J. Eng. Ind., **88**(4), pp. 393–399.
[6] Engel, P. A., 1976, *Impact Wear of Materials*, Elsevier Scientific Publishing Company, Amsterdam-Oxford-New York.
[7] Johnson, K. L., 1985, *Contact Mechanics*, Cambridge University Press, Cambridge.
[8] Janssen, M., Zuidema, J., and Wanhill, R., 2004, *Fracture Mechanics*, 2nd ed., Spon Press, Abingdon, Oxfordshire.
[9] Bourke, M. C., and Viles, H. A., 2017, "Aeolian Features," *A Photographic Atlas of Rock Breakdown Features in Geomorphic Environments*, J. A. Brearley, M. C. Bourke, H. A. Viles and R. Haas, eds., Planetary Science Institute, Tucson, pp. 6–22.
[10] Knight, J., 2008, "The Environmental Significance of Ventifacts: A Critical Review," Earth Sci. Rev., **86**(1–4), pp. 89–105.
[11] Laity, J. E., 2009, "Landforms, Landscapes, and Processes of Aeolian Erosion," *Geomorphology of Desert Environments*, Parsons, A. J., Abrahams, A. D., eds., Springer, The Netherlands, Dordrecht, pp. 597–627.
[12] Durand, M., and Bourquin, S., 2013, "Criteria for the Identification of Ventifacts in the Geological Record: A Review and New Insights," C. R. Geosci., **345**(3), pp. 111–125.
[13] Goudie, A. S., 2007, "Mega-yardangs: A Global Analysis," Geography Compass, **1**(1), pp. 65–81.
[14] Laity, J., 2008, *Deserts and Desert Environments*, Environmental systems and global change series, Vol. 2. Wiley-Blackwell, Chichester UK; Hoboken, NJ.
[15] Greeley, R., and Iversen, J. D., 1985, *Wind As a Geological Process: on Earth, Mars, Venus and Titan*, Cambridge University Press, Cambridge.
[16] Carr, M. H., 2006, *The Surface of Mars*, Cambridge Planetary Science Series, Cambridge University Press, Cambridge, New York.
[17] Laity, J. E., and Bridges, N. T., 2009, "Ventifacts on Earth and Mars: Analytical, Field, and Laboratory Studies Supporting Sand Abrasion and Windward Feature Development," Geomorphology, **105**(3–4), pp. 202–217.
[18] Greeley, R., Leach, R. N., Williams, S. H., White, B. R., Pollack, J. B., Krinsley, D. H., and Marshall, J. R., 1982, "Rate of Wind Abrasion on Mars," J. Geophys. Res.: Solid Earth, **87**(B12), pp. 10009–10024.
[19] Wang, Z.-T., Wang, H.-T., Niu, Q.-H., Dong, Z.-B., and Wang, T., 2011, "Abrasion of Yardangs," Phys. Rev. E, **84**(3), p. 031304.
[20] Ning, W.-X., Huang, X.-Q., Wang, X.-S., Li, Q., and Wang, Z.-T., 2019, "Abrasion Rates of Ventifacts," SN Appl. Sci., **1**(8), p. 855.
[21] Barber, J. R., 2018, *Contact Mechanics*, Solid Mechanics and Its Applications, Vol. 250, Springer, Cham.
[22] Finnie, I., 1995, "Some Reflections on the Past and Future of Erosion," Wear, **186–187**(Part 1), pp. 1–10.
[23] Meng, H., and Ludema, K., 1995, "Wear Models and Predictive Equations: Their Form and Content," Wear, **181–183**(Part 2), pp. 443–457.
[24] Roisman, I. V., and Tropea, C., 2015, "Impact of a Crushing Ice Particle Onto a Dry Solid Wall," Proc. R. Soc. A: Math. Phys. Eng. Sci., **471**(2183), pp. 20150525.
[25] Perez, N., 2016, *Fracture Mechanics*, 2nd ed., Springer, Switzerland.